respectively. The largest changes are the repositioning of H1 (RMSD = 10.1 Å) and an opening of CC1 in the coiled-coil next to the MTBD (RMSD = 8.1 Å) (Fig. 2, A to D, and movies S1, S2, S3, and S6), a movement anchored at the proline kink present in CC1. The final position of H1 is stabilized by multiple interactions with an acidic patch in H12 of β-tubulin not fully occupied in the low-affinity state (fig. S5A). This patch also stabilizes the high-affinity state of kinesin (*29*).

We monitored hydrogen bonds and salt bridges formed between the MTBD and the MT during MD simulations (tables S1 and S2); the high-affinity MTBD formed more hydrogen bonds with the MT (fig. S6) and electrostatic interactions at H1, H3, and H6 (fig. S5 and table S1). Nearly all of these residues are highly conserved, and mutating them results in defects in MT binding (*18*, *30*) (fig. S5). The importance of salt bridges to the MTBD-MT interaction is consistent with the sensitivity of dynein's motility to ionic strength (fig. S7).

Our structural analysis suggested that the MTBD contains residues that lower its own affinity for the MT. In the MD simulations, basic residues in H1 and H6 formed salt bridges that alternated between intramolecular and intermolecular partners. In the MT-bound high-affinity conformation, H1-K3298 switched between a glutamate on β-tubulin and a conserved glutamate in CC1 (E3289) (Fig. 3A and fig. S8A); neither contact can be formed by H1-K3298 in the low-affinity conformation (Fig. S5A). H6-R3382 switched from an intramolecular interaction with a conserved glutamate in the same helix (H6-E3378) in the low-affinity unbound state to an intermolecular interaction with a cluster of glutamates on α-tubulin upon binding (Fig. 3B and fig. S8B); the intramolecular interaction might weaken the MTBD-MT interaction in both the low- and high-affinity conformations. The importance of the two MTBD glutamates involved in the intramolecular salt bridges had previously been recognized; substitution of CC1-E3289 and H6-E3378 with alanine increased dynein's MT-binding affinity (*18*, *30*) and reduced its ATP-stimulated release from MTs, respectively (*30*). We hypothesized that these phenotypes resulted from the competition between MT and MTBD residues in CC1 and H6 for salt-bridge formation with the basic residues K3298 and R3382 in the MTBD.

To test this prediction, we mutated the residues equivalent to E3289 and E3378 in CC1 and H6 of *Saccharomyces cerevisiae* dynein to either an isosteric but neutral (Q) or a basic amino acid (K) to disrupt the salt bridge (Q) or introduce an intramolecular charge repulsion (K) that may favor intermolecular interactions between H1-K3298 or H6-R3382 and acidic residues on the MT surface. Single-molecule motility assays that monitored the movement of purified mutant dyneins showed significant increases in dynein's run length and small decreases in velocity that paralleled the severity of the mutation (E → Q → K) (Fig. 4, A and B, and fig. S9). Most notably, the basic substitutions CC1-E3289K and H6-E3378K increased dynein's run length by fivefold and sixfold, respectively (Fig. 4B), and the double mutant increased the run length even further (fig. S10). These results suggest that cytoplasmic dynein has been selected for submaximal processivity. The effects observed with the mutants are not due to a strengthened interaction with the unstructured C-terminal tails of tubulin (E-hooks). Although their removal decreased the run length of all constructs tested, in agreement with previous studies (*31*), the trend of increasing processivity (wild type → E3289K → E3378K) remained (fig. S11).

These findings provide a molecular model for how dynein couples its affinity for MTs with the nucleotide state of the motor domain (Fig. 4, C to E, and movie S6). We describe the transition from low to high affinity, but suggest that the proposed changes are reversible. During a diffusive search for its next binding site (Fig. 4C), an unbound MTBD is in the low-affinity conformation with its stalk in the β+ registry, H1 oriented perpendicular to the MT axis and intramolecular salt bridges at key MT-binding residues. Consistent with this, a nuclear magnetic resonance study found that an unconstrained, minimal MTBD in solution exists in the β+ registry and displays low affinity for MTs (*32*). Upon binding (Fig. 4D), transition to a high-affinity conforma-

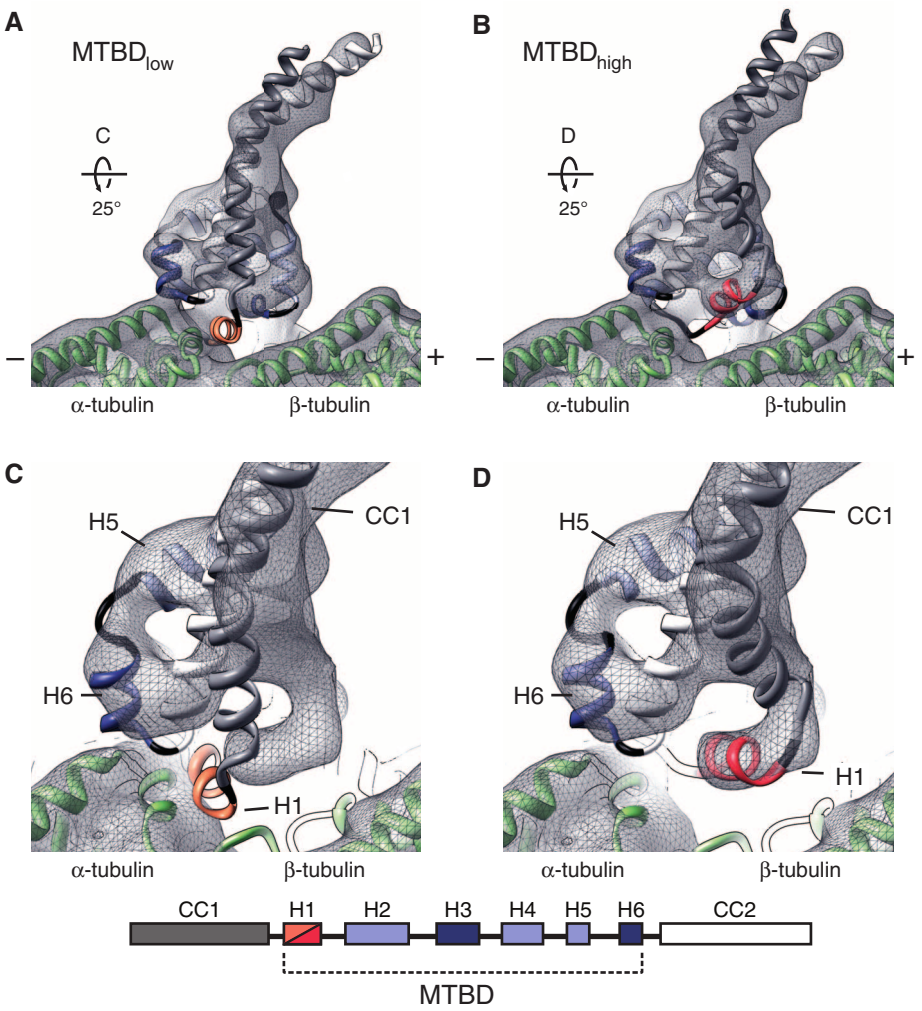

Fig. 2. The high-affinity, MT-bound state of the dynein MTBD is characterized by repositioning of helices H1 and CC1. (**A**) Rigid-body docking of the low-affinity MTBD structure into our cryo-EM density. (**B**) Pseudo-atomic model of the high-affinity MTBD bound to MTs generated by MDFF and TMD (see text for details). (**C**) Enlargement of the structure shown in (A), with its orientation indicated in (A). (**D**) Enlargement of the structure shown in (B), with its orientation indicated in (B). The cryo-EM map is shown as a transparent gray mesh. The MTBD is colored according to the scheme shown at the bottom of the figure, and structural elements are indicated in the different views. H1 (orange/red) is the element with the largest movement in the transition to the high-affinity conformation; H3 and H6 (dark blue) are major contact points with the MT (green). α- and β-tubulin are indicated (green). MT polarity is indicated in (A) and (B). H1 protrudes from the cryo-EM map and clashes with the MT in the rigid-body docked low-affinity state (A and C).